



Electronic Delocalization and Reactivity Descriptors of Quinoxaline–Triazole Systems: A Comparative HOMO–LUMO Study (QT-1 to QT- 10)

Zeba Alam¹, Ajay Kumar¹, Md Shaklain^{1,2} and Md. Serajul Haque Faizi¹

¹PG Department of Chemistry, LS College B.R.A. Bihar University, Muzaffarpur 842001

² Department of Chemistry Suresh Gyan Vihar University (SGVU) Jaipur, Rajasthan, India. 302017

Abstract

A series of quinoxaline–triazole-based Schiff base derivatives has been designed to investigate the effect of π -conjugation on electronic structure and reactivity. The present compound, a phenyl-substituted quinoxaline–1,2,4-triazole hybrid linked via an azomethine ($-\text{CH}=\text{N}-$) bridge, represents the simplest member of the series and serves as a reference system. Structurally, the molecule integrates a quinoxaline donor unit with a 1,2,4-triazole acceptor core, while the terminal phenyl group provides limited π -extension compared to higher polycyclic analogues. The relatively planar framework allows moderate delocalization of electron density across the conjugated pathway; however, the absence of extended fused aromatic systems restricts charge transfer efficiency. Consequently, this compound is expected to exhibit a comparatively larger HOMO–LUMO energy gap and lower global softness, indicating reduced chemical reactivity and enhanced stability. Such characteristics make it an ideal benchmark for evaluating the influence of increasing aromatic size in related derivatives (e.g., fluorene, anthracene, pyrene, and coronene substitutions). Overall, this study highlights the critical role of terminal aromatic substituents in tuning the electronic and structural properties of quinoxaline–triazole Schiff base systems, with potential implications for their application in optoelectronic and molecular electronic materials.

Keywords: fluorene, anthracene, pyrene, and coronene substitutions, 1,2,4-triazole, quinoxaline.

1. Introduction

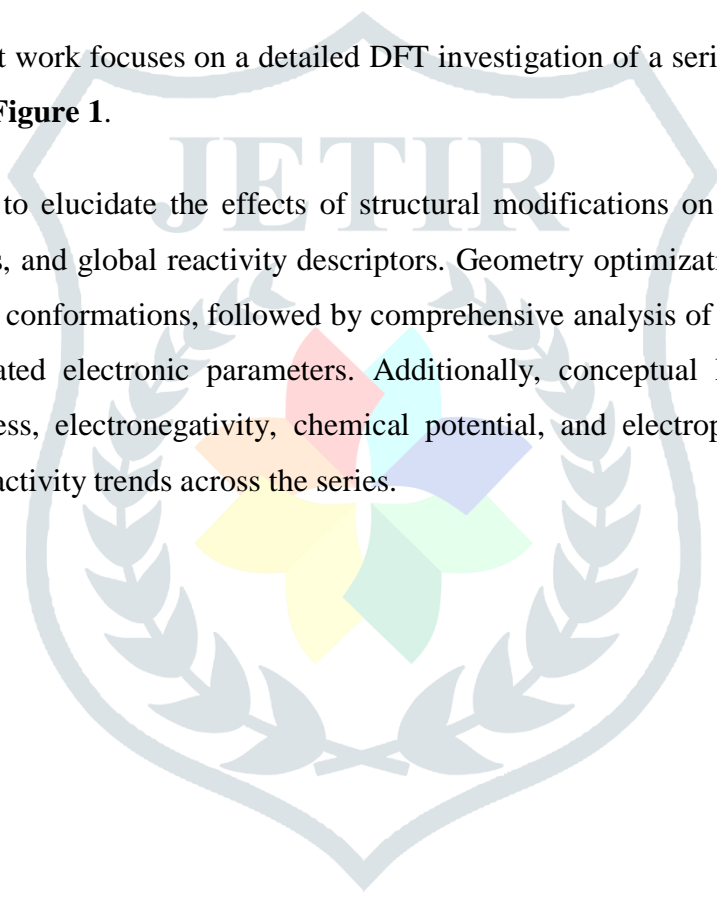
Quinoxaline-based heterocycles have emerged as a prominent class of nitrogen-containing aromatic systems owing to their remarkable electronic versatility, structural rigidity, and wide-ranging applications in medicinal chemistry, materials science, and molecular electronics. [1-10] The quinoxaline scaffold,

consisting of a fused benzene and pyrazine ring, provides an extended π -conjugated framework that facilitates efficient charge delocalization and tunable electronic properties. This inherent electronic richness has motivated extensive investigations into quinoxaline derivatives for applications such as antimicrobial, anticancer, and optoelectronic agents. In parallel, 1,2,4-triazole moieties represent another important class of heterocycles characterized by high nitrogen density, strong electron-withdrawing ability, and excellent coordination potential.[11-12] The incorporation of triazole units into conjugated systems often leads to enhanced stability, improved electron transport characteristics, and increased biological activity. The strategic fusion or coupling of quinoxalines and triazole motifs into a single molecular architecture creates a unique platform for modulating electronic structure and reactivity. Such hybrid systems are particularly attractive because they combine the π -delocalization capability of quinoxaline with the electron-deficient nature of the triazole ring, resulting in synergistic effects on molecular orbitals, charge distribution, and chemical reactivity. These structural features are expected to significantly influence key physicochemical properties, including HOMO–LUMO energy gaps, ionization potentials, electron affinities, and global reactivity descriptors. Despite the growing interest in individual quinoxaline and triazole derivatives, systematic theoretical investigations focusing on their combined frameworks remain relatively limited. In recent years, Density Functional Theory (DFT) has become an indispensable tool for exploring the electronic structure and reactivity of organic and heterocyclic compounds. [13-15] DFT-based approaches provide reliable insights into molecular geometry optimization, frontier molecular orbital (FMO) analysis, and the evaluation of global and local reactivity descriptors such as chemical hardness (η), softness (S), electronegativity (χ), electrophilicity index (ω), and chemical potential (μ). These descriptors, derived from conceptual DFT, enable a deeper understanding of structure–property relationships and allow prediction of chemical behavior in terms of nucleophilicity, electrophilicity, and stability. Furthermore, the analysis of electron density distribution and delocalization patterns offers valuable information regarding intramolecular charge transfer (ICT) processes and conjugation efficiency. Electronic delocalization plays a crucial role in determining the stability and reactivity of heterocyclic systems. In conjugated molecules, delocalization of π -electrons lowers the overall energy of the system and enhances its chemical stability, while also affecting optical and electronic properties. The degree of delocalization is often reflected in the HOMO–LUMO energy gap, where smaller gaps indicate higher polarizability, increased chemical reactivity, and improved charge transfer characteristics. For quinoxaline–triazole hybrids, the interplay between electron-donating and electron-withdrawing substituents, as well as the nature of linker units, can significantly alter the extent of delocalization across the molecular framework. Another important aspect in understanding the chemical behavior of such systems is the evaluation of global reactivity descriptors. Chemical hardness (η) and softness (S) are key indicators of molecular stability and reactivity, where hard molecules tend to resist charge transfer, while soft molecules are more reactive and polarizable. Similarly, electronegativity (χ) and chemical potential (μ) provide insights into the tendency of a molecule to attract electrons, whereas the electrophilicity index (ω) quantifies the stabilization energy upon acquiring additional electronic charge. These descriptors are particularly useful in predicting reactive sites and understanding reaction mechanisms at a molecular level. In addition to global descriptors, the analysis of frontier molecular orbitals offers a direct visualization of electron distribution in the highest occupied

molecular orbital (HOMO) and lowest unoccupied molecular orbital (LUMO). The spatial distribution of these orbitals provides critical information about electron-donating and electron-accepting regions within a molecule. For quinoxaline–triazole systems, the localization of HOMO on electron-rich regions and LUMO on electron-deficient segments may indicate efficient intramolecular charge transfer pathways, which are essential for applications in organic electronics and photonic devices. Although several studies have reported the synthesis and biological evaluation of quinoxaline and triazole derivatives, there remains a significant gap in understanding how structural variations influence electronic delocalization and reactivity descriptors in their hybrid systems. In particular, a systematic comparative study involving a series of quinoxaline–triazole compounds with varying substituents can provide valuable insights into the relationship between molecular structure and electronic behavior. Such studies are crucial for rational molecular design and optimization of functional properties.

In this context, the present work focuses on a detailed DFT investigation of a series of quinoxaline–triazole systems (QT-1 to QT-10) **Figure 1**.

The primary objective is to elucidate the effects of structural modifications on electronic delocalization, frontier molecular orbitals, and global reactivity descriptors. Geometry optimizations have been performed to obtain stable molecular conformations, followed by comprehensive analysis of HOMO–LUMO energies, energy gaps, and associated electronic parameters. Additionally, conceptual DFT descriptors such as chemical hardness, softness, electronegativity, chemical potential, and electrophilicity index have been calculated to assess the reactivity trends across the series.



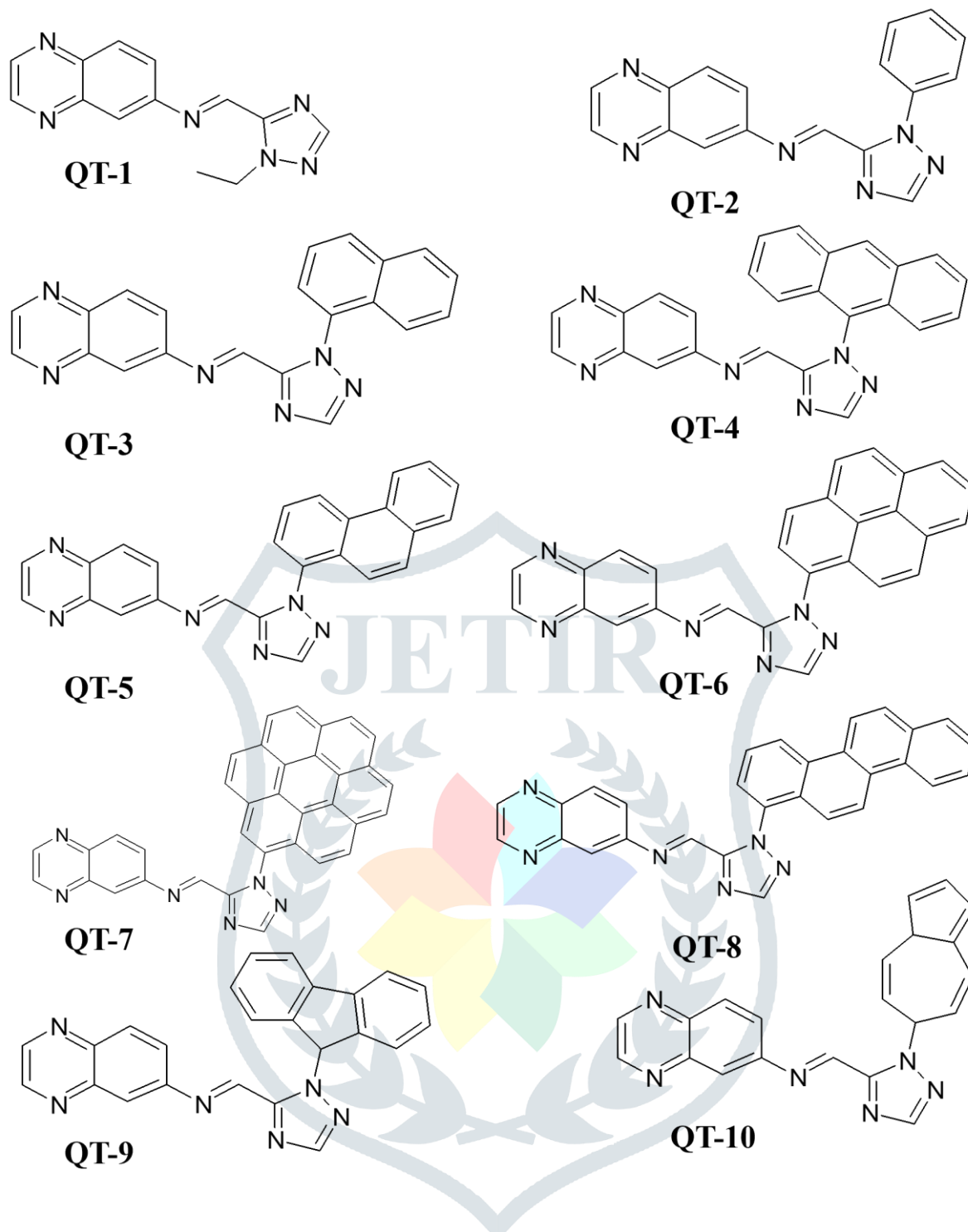


Figure 1. Series of synthesized quinoxaline triazole derivatives (QT-1–QT-10) showing structural modification through different ring substituent on the triazoles ring.

Through this comparative study, we aim to establish clear correlations between molecular structure, electronic distribution, and chemical reactivity in quinoxaline–triazole hybrids. The findings of this work are expected to contribute to a deeper understanding of electronic structure modulation in heterocyclic systems and to provide a theoretical foundation for the design of novel compounds with tailored properties for applications in medicinal chemistry and advanced functional materials.

2. Results and discussion

2.1 Structural Discussion of QT-1 to QT-10

The optimized geometries (**Figure.2**) of the quinoxaline–triazole systems- (Quinoxalin-2-yl)methylene-1,2,4-triazole derivative QT1 (Quinoxalin-2-yl)methylene-(phenyl-substituted 1,2,4-triazole) QT2- (Quinoxalin-2-yl)methylene-(naphthyl-substituted 1,2,4-triazole) QT3- (Quinoxalin-2-yl)methylene-(anthracenyl-substituted 1,2,4-triazole) QT4- (Quinoxalin-2-yl)methylene-(phenanthren-substituted 1,2,4-triazole) QT5- (Quinoxalin-2-yl)methylene-(pyrenyl-substituted 1,2,4-triazole) QT6-(Quinoxalin-2-yl)methylene-(coronenyl-substituted 1,2,4-triazole) QT7- (Quinoxalin-2-yl)methylene-(tetracenyl-substituted 1,2,4-triazole) QT8-(Quinoxalin-2-yl)methylene-(fluorenyl-substituted 1,2,4-triazole) QT9- (Quinoxalin-2-yl)methylene-(benzocycloheptenyl-substituted 1,2,4-triazole) QT10. (QT-1 to QT-10) reveal that all molecules adopt predominantly non-planar to moderately twisted conformations, governed by steric interactions between the quinoxaline core, the triazole linker, and the appended aromatic substituents. In simpler derivatives such as QT-1 and QT-2, the molecular framework remains relatively planar, facilitating effective π -conjugation between the quinoxaline and triazole units. However, as bulkier polyaromatic substituents are introduced (QT-3 to QT-10), significant torsional deviations are observed, particularly around the C–N and N–N linkages connecting the heterocyclic fragments. showing structural modification through different ring substituent on the triazoles ring. These torsions reduce coplanarity but do not completely disrupt conjugation, indicating partial electronic communication across the molecular backbone. The quinoxaline moiety consistently retains a rigid planar geometry, acting as the primary π -electron donor/acceptor scaffold, while the triazole ring functions as a conjugative bridge modulating electron density distribution. The complete density functional theory calculations with DFT/B3LYP under 6 311++G(d,p) basis set were performed using the Gaussian 09 program [16] package and GaussView 5.0. program [17].

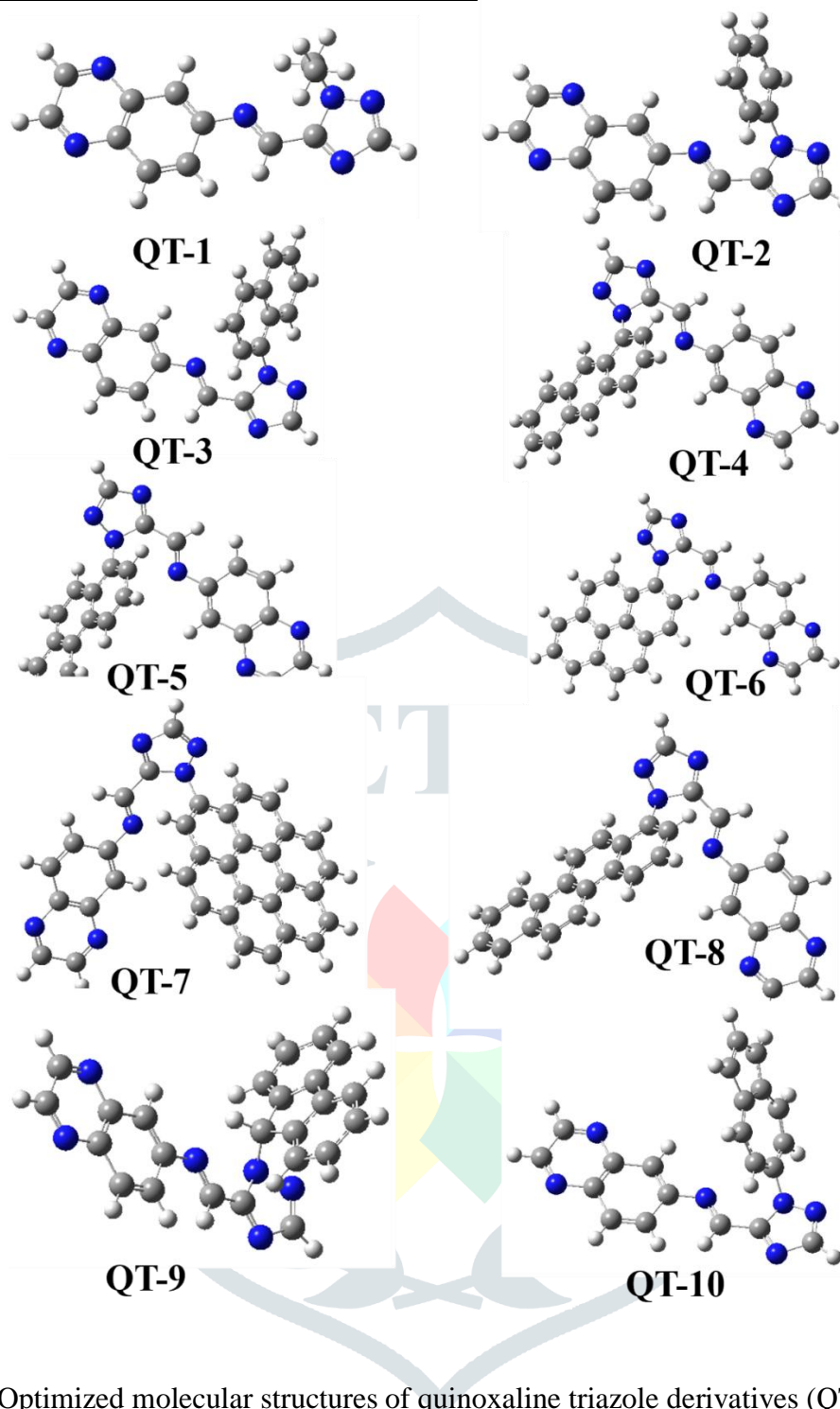


Figure 2.Optimized molecular structures of quinoxaline triazole derivatives (QT-1–QT-10)

The frontier molecular orbital (FMO) analysis provides deeper insight into electronic delocalization across the series. The HOMO is predominantly localized over the quinoxaline ring and, in some cases, extends toward the triazole linker, indicating that electron density originates mainly from the electron-rich heteroaromatic core. In contrast, the LUMO is largely distributed over the triazole unit and the attached aromatic substituents, especially in derivatives containing extended π -systems (QT-6 to QT-10). This spatial separation between HOMO and LUMO suggests efficient intramolecular charge transfer (ICT) from the quinoxaline donor region to the triazole–substituent acceptor region. Notably, compounds bearing larger conjugated substituents exhibit more diffuse and delocalized LUMO distributions, reflecting enhanced electron-accepting capability and reduced HOMO–LUMO energy gaps. [18].**Figure 3** Conversely, smaller substituents lead to more localized orbitals and relatively higher energy gaps, indicating lower polarizability. Overall, the structural variations across QT-1 to QT-10 demonstrate a clear relationship

between molecular conformation, degree of conjugation, and electronic distribution, highlighting the critical role of substituent size and orientation in tuning the electronic properties of quinoxaline–triazole systems.

Density Functional Theory (DFT) Analysis

The electronic structure of the quinoline derivatives (QT-1–QT-10) was analyzed using frontier molecular orbital (FMO) energies and derived global reactivity descriptors. The HOMO and LUMO energies were utilized to evaluate ionization potential, electron affinity, chemical hardness (η), softness (S), electronegativity (χ), electrophilicity (ω), and chemical potential (μ). The HOMO–LUMO energy gap (ΔE) plays a crucial role in determining molecular reactivity. QT-10 exhibits the smallest energy gap (7.92 eV), indicating enhanced chemical reactivity and strong intramolecular charge transfer (ICT), whereas QT-1 shows the largest gap (10.38 eV), suggesting greater kinetic stability. The chemical hardness (η) and softness (S) values further support this trend, where QT-10 and QT-4 display lower hardness and higher softness, indicating increased polarizability and reactivity. In contrast, QT-1 and QT-2 possess higher hardness values, reflecting their stable nature. **Table 2.** The electrophilicity index (ω) reveals that QT-1 is the strongest electrophile, while QT-10 exhibits relatively lower electrophilic character. This suggests that QT-1 may act as an efficient electron acceptor in chemical and biological systems. The chemical potential (μ), which represents the escaping tendency of electrons, ranges from -4.02 to -2.82 eV. QT-1 exhibits the most negative μ value, indicating higher stability and lower reactivity, whereas QT-4 shows the least negative value, suggesting enhanced electron-donating ability and chemical reactivity. The trend in μ is consistent with electronegativity and inversely related to softness, confirming the reliability of the theoretical calculations.[19]. Overall, the results demonstrate that substituent effects significantly influence the electronic distribution, allowing fine-tuning of stability, reactivity, and charge transfer properties. Compounds such as QT-10 and QT-4 are promising candidates for optoelectronic and biological applications due to their lower energy gap, higher softness, and favorable chemical potential.

Discussion of HOMO–LUMO Energies and Energy Gaps

The calculated frontier molecular orbital energies of the quinoxaline–triazole derivatives (QT-1 to QT-10) provide significant insight into their electronic structure, stability, and reactivity. The HOMO energies range from -9.21 eV (QT-1) to -6.83 eV (QT-4), indicating a gradual destabilization of the highest occupied molecular orbital with structural modification and increasing conjugation. Compounds with less negative HOMO energies (e.g., QT-4 and QT-10) exhibit enhanced electron-donating ability, suggesting that these systems can more readily participate in charge-transfer processes. In contrast, QT-1 and QT-2, with more negative HOMO energies, are comparatively more stable and less prone to electron donation.

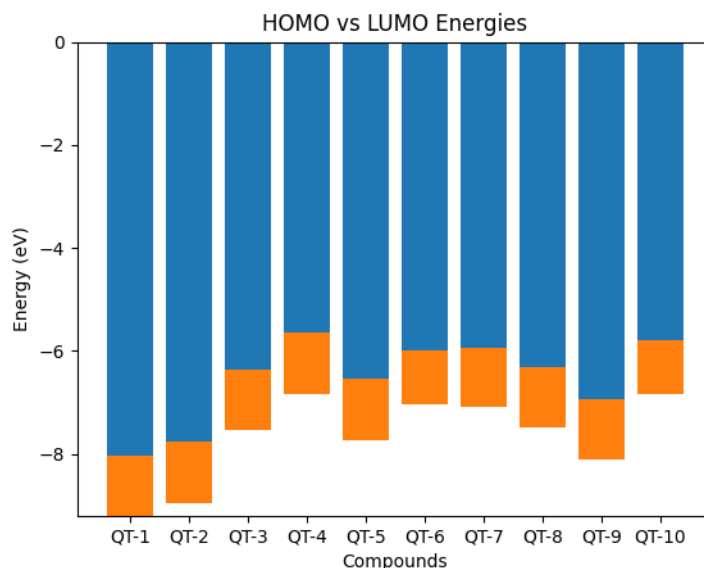


Figure 3. Bar diagram representing HOMO and LUMO energies of quinoline derivatives (QT-1–QT-10).

The LUMO energies remain relatively less variable across the series (1.03 to 1.20 eV), indicating that the electron-accepting ability is moderately influenced by substituent effects. However, a slight stabilization of LUMO is observed in QT-6 (1.03 eV) and QT-10 (1.07 eV), which may be attributed to increased delocalization over extended π -systems and electron-withdrawing regions. [20]. **Figure 4** This stabilization enhances the ability of these molecules to accept electrons, thereby facilitating intramolecular charge transfer (ICT).

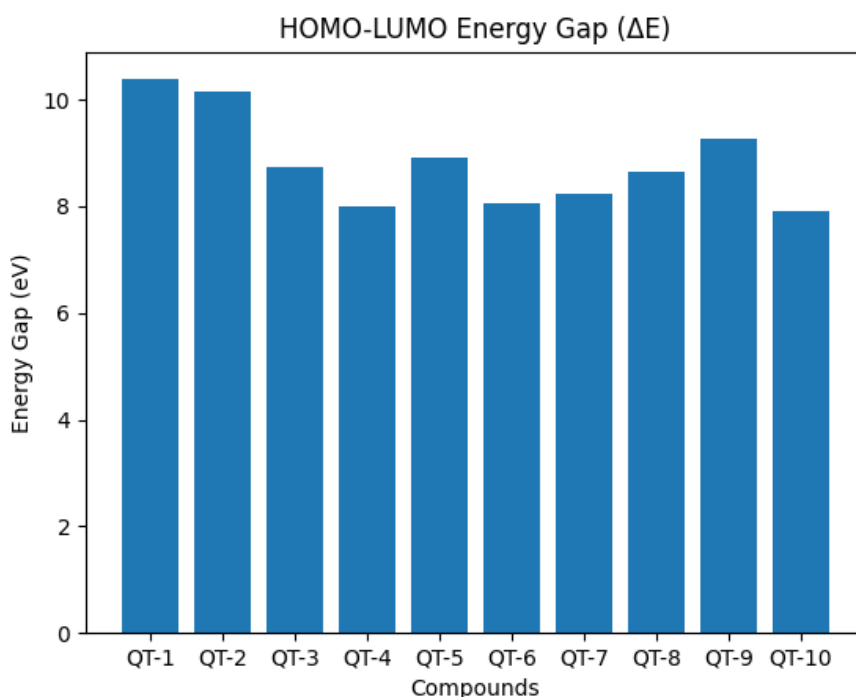


Figure 4. Bar diagram showing HOMO–LUMO energy gap (ΔE) illustrating the relative chemical reactivity.

The HOMO–LUMO energy gap (ΔE) shows a clear decreasing trend from QT-1 (10.38 eV) and QT-2 (10.16 eV) to QT-4 (8.01 eV) and QT-10 (7.92 eV), with minor fluctuations among intermediate compounds. The reduction in energy gap is indicative of increased π -electron delocalization and improved electronic communication between the quinoxaline donor and triazole acceptor units. Smaller ΔE values correspond to higher chemical reactivity, lower kinetic stability, and greater polarizability. In this context, QT-10 exhibits the lowest energy gap, suggesting it is the most reactive and electronically soft molecule in the series, while QT-1 and QT-2 are the most stable and least reactive.

Overall, the observed trends confirm that structural modifications, particularly the introduction of larger conjugated substituents, play a crucial role in tuning the electronic properties of quinoxaline–triazole systems. **Figure 5** [21]. The progressive narrowing of the HOMO–LUMO gap across the series highlights enhanced intramolecular charge transfer and suggests potential applicability of these compounds in optoelectronic and charge-transport materials.

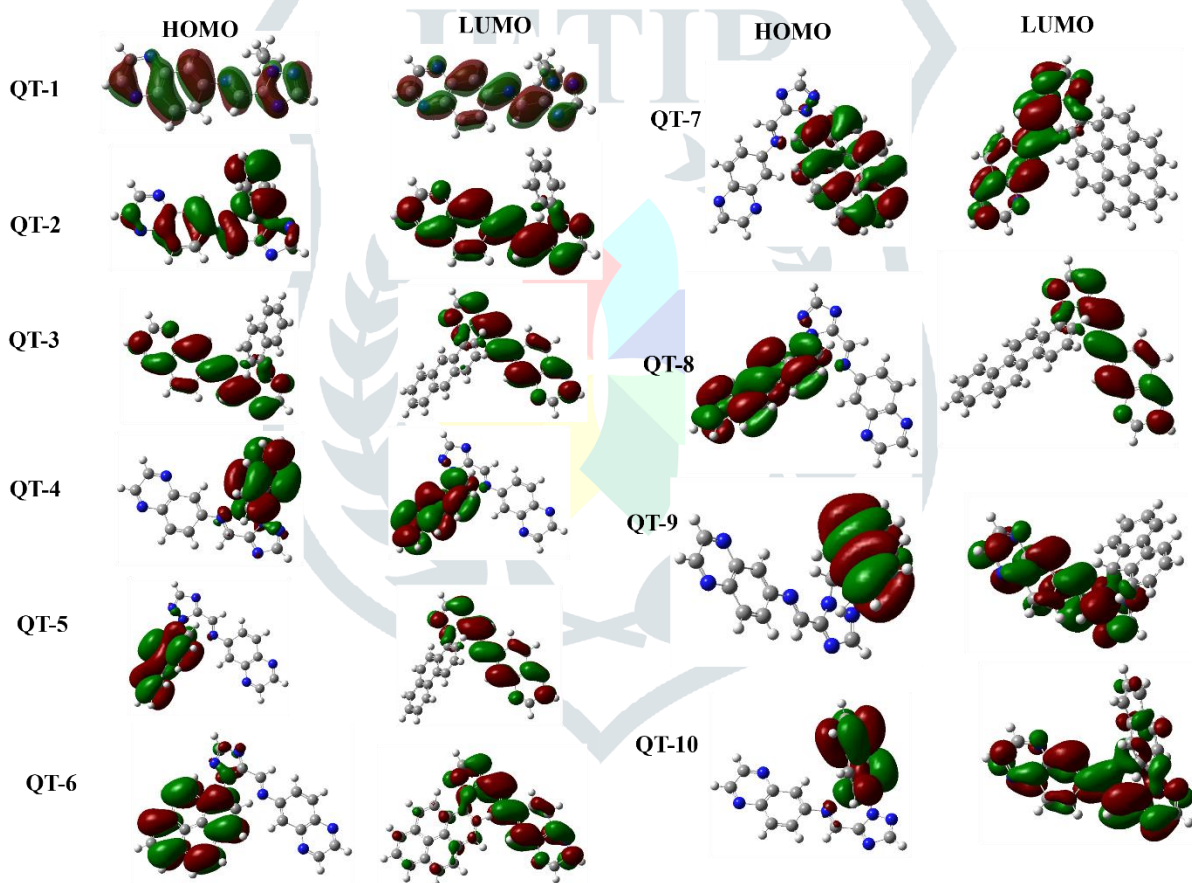


Figure 5. Frontier molecular orbitals (LUMO and HOMO) of selected quinoxaline triazole derivatives (QT-1–QT-10) illustrating electron density distribution across the molecules.

Discussion of Global Reactivity Descriptors (QT-1 to QT-10)

The global reactivity descriptors presented in Table (QT-1 to QT-10) provide comprehensive insight into the electronic stability, charge-transfer ability, and chemical reactivity of the quinoxaline–triazole systems. The ionization potential (I) shows a decreasing trend from QT-1 (9.21 eV) to QT-4 (6.83 eV), with slight fluctuations thereafter, indicating that electron removal becomes progressively easier in substituted systems

with extended conjugation. In contrast, the electron affinity (A) remains relatively consistent across the series (−1.03 to −1.20 eV), suggesting that the electron-accepting capability is moderately influenced by structural variations but does not undergo drastic changes. This balance between ionization potential and electron affinity reflects the dual donor–acceptor nature of the quinoxaline–triazole framework. Chemical hardness (η) decreases from QT-1 (5.19 eV) to QT-10 (3.96 eV), indicating a gradual transition from more stable, less reactive systems to softer and more reactive molecules. Correspondingly, the softness (S) increases from 0.193 (QT-1) to 0.253 (QT-10), **Figure 6** confirming enhanced polarizability and improved charge-transfer capability in the latter compounds **Table 1-2** This trend strongly correlates with the increasing structural complexity and conjugation in QT-6 to QT-10, where larger substituents promote electron delocalization and reduce resistance to charge redistribution.

Table 1. Calculated HOMO–LUMO Energy Gaps

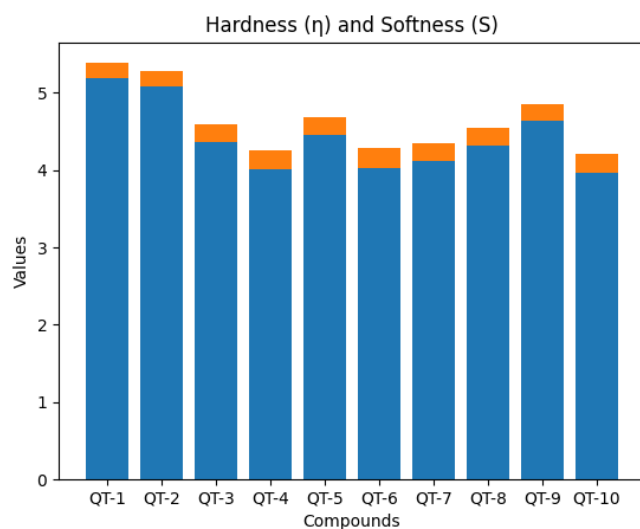
Compounds	HOMO (eV)	LUMO (eV)	ΔE (eV)
QT-1	-9.21	1.17	10.38
QT-2	-8.96	1.20	10.16
QT-3	-7.54	1.18	8.72
QT-4	-6.83	1.18	8.01
QT-5	-7.73	1.19	8.92
QT-6	-7.03	1.03	8.06
QT-7	-7.08	1.14	8.22
QT-8	-7.48	1.16	8.64
QT-9	-8.10	1.17	9.27
QT-10	-6.85	1.07	7.92

Electronegativity (χ) and chemical potential (μ) exhibit parallel trends, with χ decreasing from 4.02 eV (QT-1) to 2.82–2.89 eV (QT-4 and QT-10), while μ becomes less negative across the series. This indicates a reduced tendency of the molecules to attract electrons, which is consistent with increased electron delocalization and donor character in highly substituted derivatives. [22-29]. The electrophilicity index (ω), an important descriptor of stabilization upon electron acceptance, follows a decreasing trend from QT-1 (1.56 eV) to QT-4 (0.99 eV), with moderate variations in the remaining compounds. Higher ω values in QT-1 and QT-2 suggest stronger electrophilic nature, whereas lower values in QT-4 and QT-10 indicate reduced electrophilic reactivity and enhanced nucleophilic tendencies.

Overall, the data reveal a clear structure–property relationship across the series: early compounds (QT-1 to QT-3) are characterized by higher hardness, electronegativity, and electrophilicity, indicating greater stability and lower reactivity, while later compounds (QT-6 to QT-10) exhibit increased softness, reduced hardness, and lower energy gaps, making them more reactive and suitable for charge-transfer applications.

Table 2. Computed GRP of (QT-1–QT-10)

Compounds	I	A	η	S	χ	ω	μ (eV)
QT-1	9.21	-1.17	5.19	0.193	4.02	1.56	-4.02
QT-2	8.96	-1.20	5.08	0.197	3.88	1.48	-3.88
QT-3	7.54	-1.18	4.36	0.229	3.18	1.16	-3.18
QT-4	6.83	-1.18	4.01	0.249	2.82	0.99	-2.82
QT-5	7.73	-1.19	4.46	0.224	3.27	1.20	-3.27
QT-6	7.03	-1.03	4.03	0.248	3.00	1.12	-3.00
QT-7	7.08	-1.14	4.11	0.243	2.97	1.07	-2.97
QT-8	7.48	-1.16	4.32	0.231	3.16	1.15	-3.16
QT-9	8.10	-1.17	4.64	0.215	3.46	1.29	-3.46
QT-10	6.85	-1.07	3.96	0.253	2.89	1.05	-2.89

**Figure 6.** Bar diagram of global reactivity descriptors: hardness (η) and softness (S), indicating stability and polarizability.

This systematic modulation of reactivity descriptors highlights the crucial role of substituent effects and π -conjugation in tuning the electronic properties of quinoxaline–triazole systems, providing valuable guidance for the rational design of functional materials.

Conclusion

In this study, a quinoxaline–1,2,4-triazole Schiff base bearing a phenyl substituent was examined as the fundamental model within a series of π -conjugated derivatives. The molecular framework, consisting of a quinoxaline donor unit connected to a triazole acceptor via an azomethine linkage, exhibits moderate planarity and limited π -electron delocalization due to the presence of a simple phenyl ring. As a result, the

compound demonstrates a relatively larger HOMO–LUMO energy gap, lower global softness, and reduced charge-transfer capability compared to its higher polycyclic analogues.

This phenyl-substituted system serves as an essential reference for understanding the progressive influence of extended aromatic substituents on electronic properties. Increasing the size and conjugation of the terminal aromatic unit is expected to enhance electron delocalization, reduce the energy gap, and improve overall reactivity and optoelectronic performance. Therefore, the present compound provides a baseline for systematic comparison and highlights the crucial role of structural modification in tuning the physicochemical behavior of quinoxaline–triazole Schiff base derivatives. These findings support the rational design of advanced π -conjugated materials for potential applications in electronic, photonic, and sensing devices.

References

- [1] Yan, L.; Liu, F.-W.; Dai, G.-F.; Liu, H.-M. *Bioorg. Med. Chem. Lett.* 2007, 17, 609.
- [2] Seitz, L. E.; Suling, W. J.; Reynolds, R. C. *J. Med. Chem.* 2002, 45, 5604.
- [3] Loriga, M.; Vitale, G.; Paglietti, G. *II Farmaco.* 1998, 53, 139.
- [4] Vitale, G.; Corona, P.; Loriga, M.; Paglietti, G. *II Farmaco.* 1998, 53, 150.
- [5] Ashry, E. S. el; Abdel-Rahman, A. A.; Rashed, N.; Rasheed, H. A. *Pharmazie* 1999, 54, 893.
- [6] Carta, A.; Paglietti, G.; Rahbar Nikookar, M. E.; Sanna, P.; Sechi, L.; Zanetti, S. *Eur. J. Med. Chem.* 2002, 37, 355.
- [7] Jaso, A.; Zarranz, B.; Aldana, I.; Monge, A. *Eur. J. Med. Chem.* 2003, 38, 791.
- [8] He, W.; Myers, M. R.; Hanney, B.; Spada, A. P.; Bilder, G.; Galzcinski, H.; Amin, D.; Needle, S.; Page, K.; Jayyosi, Z.; Perrone, M. H. *Bioorg. Med. Chem. Lett.* 2003, 13, 3097.
- [9] Toris, C. B.; Camras, C. B.; Yablonski, M. E. *Am. J. Ophthalmol.* 1999, 128, 8.
- [10] Van Rensburg, C. E.; Gatner, E. M.; Imkamp, F. M.; Anderson, R. *Antimicrob. Agents Chemother.* 1982, 21, 693.
- [11]. Bozorov, K.; Zhao, J.; Aisa, H. A. *Bioorg. Med. Chem.*, 2019, 27, 3511–3531.
- [12]. Bayomi, S. M.; Moustafa, M. A.; Maarouf, A. R.; Abutaleb, M. H. *J. Am. Sci.*, 2016, 12, 40–56.
- [13]. Foresman, J.; Frish, E. Gaussian Inc., Pittsburg, USA. 1996
- [14]. Fleming, I. *Frontier orbitals and organic chemical reactions*; Wiley. 1977.
- [15]. Yang, W.; Parr, R. G. *Proc. Natl. Acad. Sci. U. S. A.* 1985, 82, 6723.
- [16]. Frisch, M.; Trucks, G.; Schlegel, H.; Scuseria, G.; Robb, M.; Cheeseman, J.; Scalmani, G.; Barone, V.; Mennucci, B.; Petersson, G. Gaussian 09, Gaussian Inc., Wallingford. 2009.
- [17]. Dennington, R.; Keith, T.; Millam, J. GaussView 5.0, Semichem Inc., Wallingford. 2009.
- [18] Parr, R. G.; Pearson, R. G. *Absolute Hardness: J. Am. Chem. Soc.* 1983, 105, 7512–7516.
- [19] Parr, R. G.; Szentpály, L. V.; Liu, S. *J. Am. Chem. Soc.* 1999, 121, 1922–1924.
- [20]. Selby, T. P.; Denes, L. R.; Kilama, J. L.; Smith, B. K. *ACS Symposium Series 584 (1995): 171–85.*
- [21]. Saito, I.; Matsuura, T. *Biochemistry* 6, no. 11 (1967): 3602–8.
- [23]. Azuaje, J.; Maatougui, A. E.; Garcia-Mera, X.; Sotelo, E. *ACS Combinatorial Science* 16 (2014): 403–11
- [24]. Saifina, D. F.; Mamedov, V. *Russian Chemical Reviews* 79 (2010): 351–70.

[25]. Haddadin, M. J.; Issidorides, C. H. *Tetrahedron Letters* 6 (1965): 3253–6.

[26]. O'Brien, D.; Weaver, M.; Lidzey, D.; Bradley D., *Applied Physics Letters* 69 (1996): 881–3.

[27]. Ma, H.; Li, D.; Yu, W. *Organic Letters* 18, no. 4 (2016): 868–71.

[28]. Ahn, J.; Lee, S. B.; Song, I.; Chun, S.; Oh, D.; Hong, S. *The Journal of Organic Chemistry* 86, no. 11 (2021): 7390–402.

[29]. Xu, H.; Fan, L. *European Journal of Medicinal Chemistry* 46, no. 5 (2011): 1919–25.

